Version of Record: https://www.sciencedirect.com/science/article/pii/S0960148118304348
Manuscript_4ee7502a3ddc6a2afd8977262cbd684b

Non-parametric models for joint probabilistic distributions of wind speed and direction data

Qinkai Han [a], Zhuolin Hao [b], Tao Hu [b,*], Fulei Chu [a]

[a] *The State Key Laboratory of Tribology, Tsinghua University, Beijing 100084, China*

[b] *School of Mathematical Sciences, Capital Normal University, Beijing 100048, China*

Abstract

Two non-parametric models, namely the non-parametric kernel density (NP-KD) and non-parametric JW (NP-JW) models, are proposed for joint probabilistic modeling of wind speed and direction distributions. In the NP-KD model, a novel bivariate kernel density function, which could consider the characteristics of both wind direction (angular) and speed (linear) data, is firstly constructed and the optimal bandwidth is selected globally through two cross-validation (CV) methods. In the NP-JW model, the univariate Gaussian and von Mises kernel density functions are, respectively, utilized to fit the wind speed and direction data. The estimated wind speed and direction distributions are used to form the joint distribution according to the JW model. Several classical parametric models, including the AG, Weibull, Rayleigh, JW-TNW and JW-FMN models, are also introduced in order for comparisons with the proposed non-parametric models. By conducting various tests on the real hourly wind speed and direction data, the goodness of fit of both parametric and non-parametric models is compared and evaluated in detail. It is shown that the non-parametric models (NP-KD, NP-JW) generally outperform the para-

metric models (AG,Weibull,Rayleigh,JW-TNW,JW-FMN) and have more robust performance in fitting the joint speed and direction distributions. Among the two non-parametric models, the NP-KD model has better performance in fitting joint distribution, while the NP-JW model has higher accuracy in fitting the marginal speed (or direction) distributions.

Key words: non-parametric model, kernel density estimation, joint probabilistic distribution, marginal distribution

1 Introduction

With increasing climate change and environmental concerns, wind energy has now become the world's fastest growing source of renewable and green energy. Accurate estimation of wind characteristics is critical to the assessment of wind energy potential, the site selection of wind farms, and the operations management of wind power conversion systems.

Among the wind characteristics, wind speed is one of the most important parameter to be considered in the design and operations of wind energy conversion systems [1–3]. Various statistical models have been proposed and utilized for analyzing the wind speed frequency distributions with probability density functions (PDFs). The two-parameter Rayleigh and Weibull models are by far the most widely adopted for representing the wind speed [4]. Other theoretical distributions suitable for modeling the wind speed are square root normal [5], three-parameter Weibull [6], inverse Gaussian [7], etc. Be-

* Corresponding author.
Email address: hutaomath@foxmail.com (Tao Hu).

sides the classical statistical models, some new parametric models, such as Bayesian model averaging (BMA) [8], Measure-Correlate-Predict (MCP) [9], Johnson S_B distribution [10], and mixture distributions [11,12], have been put forward recently for application. Despite the extensive efforts on modeling wind speed distribution, a comprehensive and fair comparison is still not enough. Carta, Ramirez and Velazquez [13], Zhou et al. [14], respectively, compared the effectiveness of multiple statistical distributions for characterizing the wind speed for various wind sites, and used a comprehensive evaluation metric for goodness-of-fit. They found that the popular Weibull distribution cannot represent all the wind regimes encountered in nature, for example, those with high percentages of null wind speeds, bimodal distributions, etc. Ouarda, Charron and Chebana [15] introduced novel moment and L-moment ratio diagram methods for the optimal selection of probability distributions for wind speed data.

Besides the wind speed analysis, the distribution analysis of wind direction is another important aspect of wind energy assessment. Fisher [16] introduced several commonly used models for handling circular data. Currently, the von Mises distribution function is one of most popular functions for fitting the wind direction data. Carta et al. [17] first used a finite mixture of the von Mises (FMvM) distribution to characterize the wind direction for Canary Islands, Spain. Recently, Masseran et al. [18] utilized the FMvM for fitting the wind direction data of Peninsular Malaysia, and the effect of monsoon seasons on the wind direction behaviors was analyzed in detail [19]. They also constructed a new circular distribution based on nonnegative trigonometric sums for wind direction fitting. Heckenbergerova et al. [21,22] paid attention to the parameter estimation and model optimization for the FMvM distribution.

It is well known that the wind speed and direction should be treated as dependent random variables. Generally, a more realistic and complete approach is to consider the joint distribution of wind speed and direction, instead of the univariate (marginal) PDFs. Research shows that the joint probability approach could support the decision making [23], and improve the accuracy of wind energy assessment under specific cases [24]. More variables, such as wind turbulence [25], are also beginning to be considered in joint probability analysis. Some studies were directed at constructing bivariate distributions models for representing wind speed and direction simultaneously. However, compared with numerous wind speed distribution models, these models are less common. Smith [26] discussed using the bivariate Normal density function for predicting the distribution of wind speed and direction. Weber [27] developed a more flexible model by lifting the equal variance assumption, which is called the anisotropic Gaussian (AG) model. Johnson and Wehrly [28] proposed a parametric model, namely the JW model, for representing wind speed and direction by obtaining angular-linear distributions. Carta, Ramirez and Bueno [29] generalized the JW model and then proposed a flexible joint PDF of wind speed and direction, based on angular-linear distributions with specified marginal distributions that were compared with AG models. After evaluating the fitted distributions through the coefficient of determination, the authors concluded that the proposed model provided better fits for the examined cases in the Canary Islands. Erdem and Shi [30] constructed seven bivariate distributions based on three construction approaches (angular-linear, Farlie-Gumbel-Morgenstern, anisotropic lognormal) that were compared by applying the adjusted coefficient of determination and the root mean square error as goodness-of-fit measures. Four sites in North Dakota were examined as case studies and the results revealed that the anisotropic approach lags significant-

ly compared to the other two methods, which provided very close values for the two measures. Soukissian [31] implemented the same model of Carta [29] for the joint modelling of linear/directional wind and wave characteristics. Recently, Soukissian and Karathanasi [32] thoroughly examined and evaluated three families of models for the joint probabilistic description of wind speed and direction data. The obtained results suggested that the performance of the JW model is rather superior, since it provides better fits compared to the other two families of bivariate distributions for the overwhelming majority of the examined cases and criteria.

As the above literature shown, the parametric models have been widely adopted in modeling the wind speed and direction distributions. Besides the parametric models, the non-parametric models (such as the kernel density estimation, KDE) are also popular in the probabilistic modeling of wind data [33]. The most attractive feature of non-parametric models is that it directly makes use of sample data without a need of estimating characteristic parameters in a theoretical distribution [34]. In other words, there is no error caused by assumption of a theoretical distribution for wind speed and by mismatch between estimated parameters and actual behaviors of wind speed. Thus, the non-parametric models could better describe the natural characteristics of the wind speed and direction, which is conducive for the accurate estimation of wind resources at potential sites. Qin, Li and Xiong [34] proposed a non-parametric KDE method for wind speed probability distribution, and compared with ten conventional parametric models using three year's actual wind speed data at ten wind frams sites with different wind speed behaviors. Based on the diffusion partial differential equation in finite domain, Xu, Yan and Xu [35] presented an improved KDE method to account for both bandwidth selec-

tion and boundary correction problems. Ouarda et al. [36] and Wang, Hu and Ma [33] conducted comprehensive reviews and comparisons on non-parametric models for wind speed probability distribution in the UAE and central China, respectively.

Although the non-parametric models have been proved to be effective and more accurate in the probabilistic modeling of wind speed [33–36], its applications in wind direction distributions have been slow and inadequate. Until recently, Oliveira, Crujeiras and Rodriguez-Casal [37] developed a circular KDE procedure to fit the wind direction data, and provided different alternatives for choosing the bandwidth parameters. It is rare to see the non-parametric models for the joint wind speed and direction modeling in current literature. Actually, the non-parametric joint distribution model can well supplement the deficiency of the parametric model, and the assessment of wind energy potential could be benefited accordingly. Lately, Zhang et al. [38] conducted a pioneering work on the joint modeling of wind speed and direction data. They proposed a multivariate KDE model, which they called the multivariate and multimodal wind distribution (MMWD) model, to capture the coupled variation of wind speed and direction. The effectiveness and the reliability of the MMWD model were successfully validated using the ten-year wind data. However, the kernel function of the MMWD model is designed for wind speed (linear) data, and is not specially for the wind direction (angular) data. Such treatment might cause some errors in application.

A literature review indicated that only a few studies have used the non-parametric models for fitting the wind direction distributions; this is particularly true for the joint probabilistic distributions of wind speed and direction data. Moreover, there have few attempts to comprehensively compare the

performance and robustness of both parametric and non-parametric models in modeling various wind speed/direction data. Therefore, the novelty and contributions of this study can be summarised as follows:

■ A framework for modeling joint probabilistic distributions of wind speed/direction data is introduced. Two non-parametric models with univariate and bivariate kernel functions are proposed to fit joint speed/direction distributions.

■ In the non-parametric kernel density (NP-KD) model, a novel bivariate kernel density function, which could consider the characteristics of both wind direction (angular) and speed (linear) data, is firstly constructed and the optimal bandwidth is selected globally through two cross-validation (CV) methods. In the non-parametric JW (NP-JW) model, the univariate Gaussian and von Mises kernel functions are, respectively, utilized to fit the wind speed and direction data. The estimated wind speed and direction distributions are used to form the joint distribution according to the JW model.

■ Various tests on the real data from four wind sites of China are conducted. Non-parametric models generally have more accurate and robust performances than most current parametric models in joint modeling of wind speed/direction data. It is believed that the assessment of wind energy potential could be benefited accordingly.

The remainder of this paper is organised as follows. Section 2 introduces the proposed method, section 3 describes the wind data acquired from various observation sites in China, section 4 gives the parameter estimations of both parametric and non-parametric models, section 5 presents and discusses the results, and section 6 lists the conclusions of the study.

2 Models

The structures and procedures for two non-parametric models (NP-KD and NP-JW) are proposed in detail. Then, several classical parametric models, including the AG model and JW models, are briefly explained in order for comparisons. Finally, four metrics are introduced for measuring the goodness of fit.

2.1 NP-KD model

Before applying the NP-KD model, the first issue to be solved is the selection of kernel density functions. For the linear (wind speed v) data, the univariate Gaussian function is usually utilized in the non-parametric models. Its expression is given as

$$K_V(v) = \frac{1}{\sigma\sqrt{2\pi}} \exp\Big(- \frac{(v-\mu_v)^2}{2\sigma^2}\Big) \tag{1}$$

in which $\mu_v \geq 0$ represents the mean value of wind speed, and σ denotes bandwidth parameter of the univariate Gaussian function. The von Mises kernel function is used for fitting the angular (wind direction θ) data, and its expression could be written by

$$K_\Theta(\theta) = \frac{1}{2\pi I_0(\kappa)} \exp(\kappa \cos(\theta - \mu_\theta)) \tag{2}$$

in which $\mu_\theta \in [0, 2\pi)$ represents the mean value of wind direction, and κ denotes bandwidth parameter of the univariate von Mises kernel function. The $I_0(\kappa) = \sum_{m=0}^{\infty} \frac{(-1)^m}{m!\Gamma(m+1)} \Big(\frac{\kappa}{2}\Big)^{2m}$ represents the modified Bessel function of

the first kind and order zero, in which $\Gamma(\cdot)$ is the Gamma function.

Most current functions could not consider the angular (wind direction θ) and linear (wind speed v) data simultaneously. Considering the characteristics of both Gaussian and von Mises kernel functions, a novel bivariate kernel density function is constructed by multiplying the two univariate kernel density functions together. From Eqs. (1) and (2), the newly constructed bivariate kernel function could be expressed as follows

$$\begin{aligned} K_{V,\Theta}(v,\theta) &= K_V(v) \cdot K_\Theta(\theta) \\ &= \frac{1}{(2\pi)^{3/2} I_0(\kappa)\sigma} \exp\Big(- \frac{(v-\mu_v)^2}{2\sigma^2}\Big) \exp(\kappa \cos(\theta - \mu_\theta)) \end{aligned} \tag{3}$$

in which σ, κ are the two bandwidth parameters for the bivariate kernel function. They should be determined globally through the optimization algorithm, which will be introduced in the following section.

If $(v_1,\theta_1),(v_2,\theta_2),\cdots,(v_n,\theta_n)$ are random samples from unknown bivariate populations, the joint PDFs of the wind speed and direction based on the bivariate kernel density functions (NP-KD model) is expressed as follows

$$\begin{aligned} f_{V,\Theta}(v,\theta) &= \sum_{i=1}^{n} K_{V,\Theta}(v,\theta) \\ &= \frac{1}{(2\pi)^{3/2} I_0(\kappa)\sigma} \sum_{i=1}^{n} \exp\Big(- \frac{(v-\mu_i)^2}{2\sigma^2}\Big) \exp(\kappa \cos(\theta - \mu_i)) \end{aligned} \tag{4}$$

How to determine optimal values of the bandwidths σ, κ is the key problem in NP-KD model. Usually, the bandwidth values could be obtained by minimizing an error function. For instance, the mean integrated squared error (MISE) or cross validation (CV) are all alternatives. According to the result of Zambom

and Dias [39], compared with the MISE method, the CV method has some major advantages, i.e. simple implementation and robust performance. Thus, the CV method will be utilized for choosing the optimal bandwidth values σ, κ.

There are two CV methods for use, one of which is called the likelihood cross-validation (LCV). According to the idea of LCV, the optimal bandwidth is calculated by minimizing the likelihood function

$$LCV(\sigma,\kappa) = \prod_{i=1}^{n} f_{-i,V,\Theta}(v_i,\theta_i,\sigma,\kappa) \tag{5}$$

where $f_{-i,V,\Theta}$ represents the joint density estimation after deleting the ith observation value in Eq. (4). Another CV method is called the least square cross-validation (LSCV). Using the LSCV, the optimal bandwidth value is determined by minimizing the following equation as

$$LSCV(\sigma,\kappa) = \int_0^{2\pi}\int_0^{\infty} f_{V,\Theta}^2(v,\theta,\sigma,\kappa)\mathrm{d}v\mathrm{d}\theta - \frac{2}{n}\sum_{i=1}^{n} f_{-i,V,\Theta}(v_i,\theta_i,\sigma,\kappa) \tag{6}$$

From the results by Oliveira et al. [40], except for the peak distribution case, in most cases the LCV is a good bandwidth estimation method. However, the LSCV behaves more stable. In this study, both the LCV and LSCV methods are all utilized for estimating the bandwidth values, and the best results are retained.

2.2 NP-JW model

In the NP-JW model, the classical JW model will be utilized for establishing probability density for an angular-linear distribution. The expression of JW model is given by [28]

$$f_{V,\Theta}(v,\theta) = 2\pi g(\zeta) f_V(v) f_\Theta(\theta) \qquad 0 \le \theta < 2\pi, -\infty \le v < \infty \tag{7}$$

in which $f_V(v), f_\Theta(\theta)$ are PDFs of wind speed and direction, ζ represents the circular variable between the wind speed and direction, and its definition is expressed as

$$\zeta = \begin{cases} 2\pi[F_V(v) - F_\Theta(\theta)], & F_V(v) \ge F_\Theta(\theta); \\ 2\pi[F_V(v) - F_\Theta(\theta)] + 2\pi, & F_V(v) < F_\Theta(\theta). \end{cases} \tag{8}$$

where $F_V(v), F_\Theta(\theta)$ are cumulative distribution functions (CDFs) of wind speed and direction, $g(\zeta)$ denotes the PDF of ζ.

Although most current kernel function could not describe the angular and linear data at the same time, one can use the univariate Gaussian and von Mises kernel functions to fit the wind speed and direction data, respectively. Then, according to Eq. (7) of JW model, the joint density estimation results could also be gained. This is the main idea of NP-JW model, which could be considered as the non-parametric version of the JW model. The procedure of NP-JW model is expressed as follows:

(1) Univariate Gaussian and von Mises kernel functions are, respectively, used for fitting the wind speed and direction data. The corresponding cumulative

distributions for the wind speed and direction are then computed through numerical integration of the estimated density distributions.

(2) The circular variable ζ is gained using Eq. (8). As the ζ is an angular variable, the univariate von Mises kernel function is also utilized to fit $g(\zeta)$ (PDF of ζ).

(3) After the PDFs of single wind speed, direction and circular variable data obtained, then the joint density estimation results could be gained using Eq. (7).

Using two CV methods described in Eqs. (5-6), the optimal bandwidth values for the univariate Gaussian and von Mises kernel functions in NP-JW model are determined accordingly.

2.3 Several popular parametric models

One of the most popular parametric models for fitting joint wind speed and direction distributions is the AG model, which was proposed by Weber [27] in 1991. The model has some hypotheses: the wind speed components for the prevailing wind direction are random variables which are described by a Gaussian distribution; the longitudinal and lateral wind speed components are statistically independent of each other. Based on the hypotheses and the polar coordinate transformation method, the joint probability density function of wind speed and wind direction is derived accordingly. Detailed expressions could be found in Ref. [29].

The JW family is another widely adopted parametric models in joint fitting of

wind speed and direction data. Usually, the finite mixture of von Mises distributions (FMvM) are utilized for PDF modeling of random angular variables θ, ζ. For the random wind speed data, both the truncated normal-Weibull mixture distribution (TNW) and finite mixture normal distribution (FMN) are the most commonly used models. Thus, there are two JW models, namely the JW-TNW model and JW-FMN model, whose detailed expressions are given in Ref. [29].

Here, the Expectation-Maximization (EM) algorithm [41,42] is utilized to estimate the parameter values of various distributions. EM algorithm is a powerful method providing the distribution parameter estimates and it could be used as an alternative method for finding the maximum likelihood estimates. According to Banerjee et al. [41], let us suppose that the posterior distribution of the unknown parameters is known. Expectation step is computed using current estimate of parameters as the expectation of the log-likelihood method. In the maximization step, the parameter estimates are computed by maximization of the expected log-likelihood obtained in expectation step. Detailed procedure for the EM algorithm could be found in Refs. [41,42].

2.4 Model evaluation metrics

Four metrics, including root mean square error (RMSE), mean absolute error (MAE), index of agreement (IA) [14] and χ^2 statistic [43], are defined to measure the goodness of fit of both parametric and non-parametric models. RMSE is very sensitive to the large or small errors in a set of measurements, and thus it can reflect the precision of measurement very well. Compared with the mean error (ME), MAE can better measure the actual fitting error because

the offset of positive and negative errors does not appear in the MAE, and IA is a bin-specific static which resembles R^2 statistic. It is a relative figure that can take the values between 0 and 1, and a higher value indicates a better fit between the specified distribution and observed data values. χ^2 statistic is calculated from the observed and expected frequencies. If the χ^2 test value is smaller than the critical value, the hypothesis stating that the data follow the specified distribution is accepted. The test is bin-specific and the test value is dependent on how the bins are selected. χ^2 test has been extensively used to compare various statistical distributions for characterization of wind data.

Two probability values are defined here to calculate the above-mentioned four metrics. The wind speed-direction plane is divided into $k \times k$ elements. The $p_i^{(o)}$ represents the real probability value of random variables falling into the area (i, j) $(1 \leq i, j \leq k)$, while the $p_i^{(e)}$ is the probability value obtained by density estimation model. Then, the four metrics are expressed by

$$RMSE = \sqrt{\frac{1}{n} \sum_{i,j} \left(p_i^{(o)} - p_i^{(e)} \right)^2} \tag{9}$$

$$MAE = \frac{1}{n} \sum_{i,j} \left| p_i^{(o)} - p_i^{(e)} \right| \tag{10}$$

$$IA = 1 - \frac{\sum_{i,j} \left(p_i^{(o)} - p_i^{(e)} \right)^2}{\sum_{i,j} \left(\left| p_i^{(o)} - \bar{p}_i^{(o)} \right| + \left| p_i^{(e)} - \bar{p}_i^{(e)} \right| \right)^2} \tag{11}$$

$$\chi^2 = \sum_{i,j} \frac{\left(np_i^{(o)} - np_i^{(e)} \right)^2}{np_i^{(e)}} \tag{12}$$

where n denotes the total number of the wind data sample. Among the four metrics, except for the IA, the lower value of other three metrics (RMSE, MAE

and χ^2 statistic) means that the model would have higher accuracy. According to the definition of IA (see Eq. (11), one can find that the value of IA varies between 0 and 1. The value of IA is more close to 1, indicating that the model is more accurate.

3 Wind data descriptions

By employing anemometers, the wind speed and direction data could be measured and captured at a wind observation site. In this study, four wind observation sites in China are selected and shown in Fig. 1. Their geographical positions are listed in Tab. 1. The wind data in various observation sites were recorded continuously by the anemometers, and the wind attributes (including wind speed, direction, etc.) could be obtained accordingly. Tab. 1 also describes the wind data periods used in the analysis.Due to the electrical or mechanical reasons, the output wind speed of anemometers might be invalid. The data periods were carefully chosen to make sure that there is no invalid wind speeds. Thus, the completeness of data in our selected data samples is all 100%, which is shown in Tab. 1.

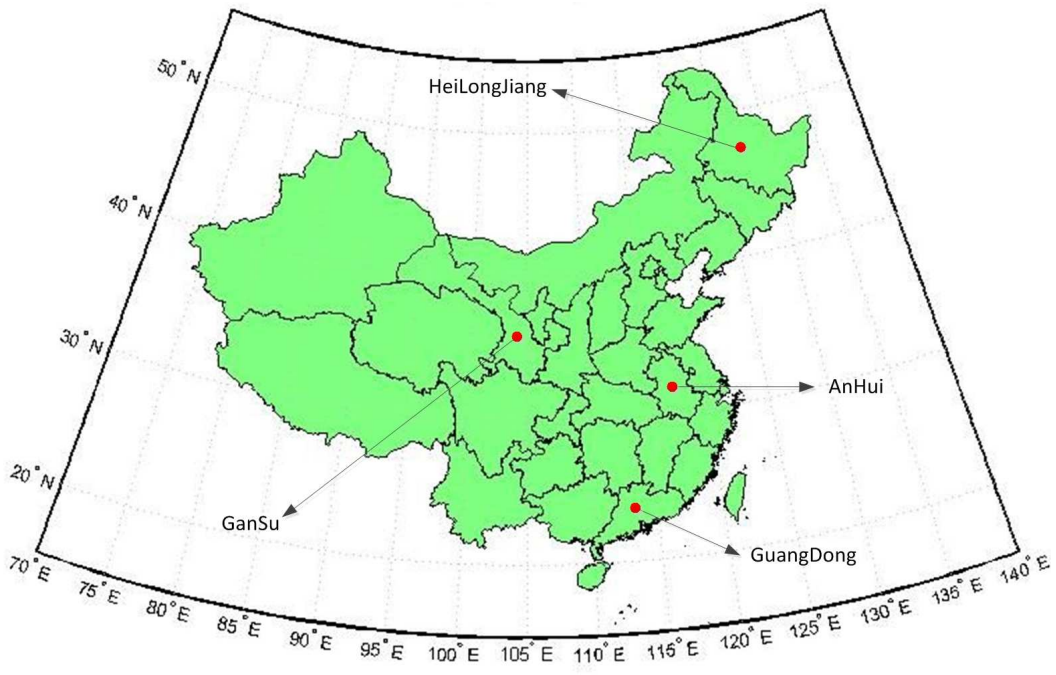

Fig. 1. Selected wind observation sites in China.

Table 1

Locations of four observation stations in China.

Observation station	Longitude	Latitude	Altitude(m)	Data period	Completeness of data
AnHui(AH)	$117^0 17^{'}$E	$31^0 52^{'}$N	20	7/8/2011-5/7/2012	100%
GuangDong(GD)	$113^0 17^{'}$E	$23^0 8^{'}$N	11	12/24/2011-2/28/2013	100%
GanSu(GS)	$103^0 44^{'}$E	$36^0 2^{'}$N	1500	1/16/2014-5/27/2014	100%
HeiLongJiang(HLJ)	$126^0 38^{'}$E	$45^0 45^{'}$N	128	11/1/2015-2/23/2016	100%

Usually, the anemometer tower records the wind speed and direction data in every 10 minutes. Although there is no restriction on the sampling time period for the proposed non-parametric models, the wind data usually needs to be treated as the hourly average data. Such treatment could reduce the unwanted fluctuation components of the wind data and also improve the calculation efficiency. The data should be treated as the hourly average data. The wind

direction starts from the North and increases clockwise. Using the vector averaging method [44], the 10-min wind directions are transformed into hourly average wind direction

$$\theta_h = \begin{cases} \arctan\left(\bar{V}_x/\bar{V}_y\right), & \bar{V}_x \geq 0, \bar{V}_y > 0; \\ \arctan\left(\bar{V}_x/\bar{V}_y\right) + \pi, & \bar{V}_x > 0, \bar{V}_y \leq 0; \\ \arctan\left(\bar{V}_x/\bar{V}_y\right) + \pi, & \bar{V}_x \leq 0, \bar{V}_y < 0; \\ \arctan\left(\bar{V}_x/\bar{V}_y\right) + 2\pi, & \bar{V}_x < 0, \bar{V}_y \geq 0. \\ 0, & \bar{V}_x = 0, \bar{V}_y = 0 \end{cases} \tag{13}$$

where $\bar{V}_x, \bar{V}_y$ are the hourly averaged wind speeds, and could be expressed as follows

$$\begin{aligned} \bar{V}_x =& \frac{1}{6}\sum_{i=1}^{6}\left(V_{m,i}\sin\theta_{m,i}\right) \\ \bar{V}_y =& \frac{1}{6}\sum_{i=1}^{6}\left(V_{m,i}\cos\theta_{m,i}\right) \end{aligned} \tag{14}$$

in which $V_{m,i}, \theta_{m,i}$ represent the 10-min wind speed and direction. After averaging the 10-min data, one obtains the absolute value of wind speed as follows

$$V_h = \sqrt{\bar{V}_x^2 + \bar{V}_y^2} \tag{15}$$

Thus, the hourly average wind speed and direction observed at four wind sites are plotted in Fig. 2.

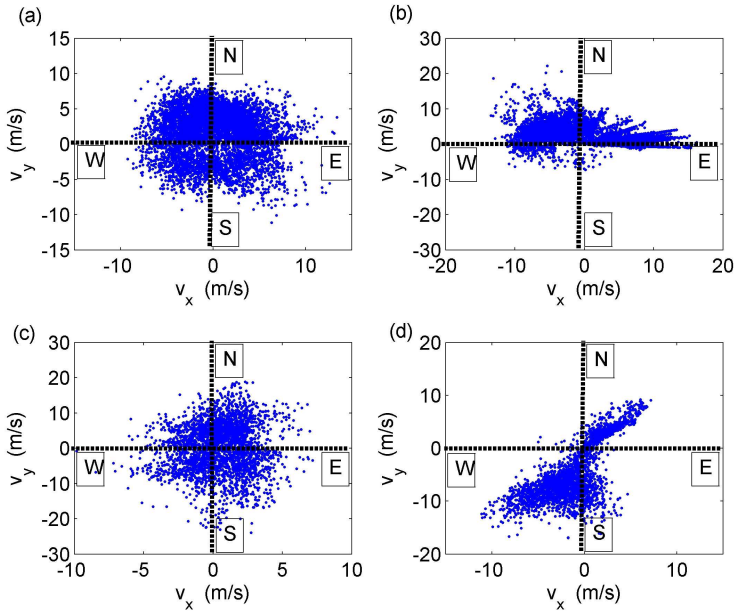

Fig. 2. Hourly average wind speed and direction observed at four wind sites: (a) AH; (b) GD; (c) GS and (d) HLJ.

4 Model parameter estimations

4.1 Parametric models

For the AG model, the parameters includes the mean and variance of the longitudinal wind speed $(\mu_{y'}, \sigma_{y'})$ and variance of the lateral wind speed $(\sigma_{x'})$. The parameters of FMvM distributions are the mean wind direction μ_i, smoothing parameter κ_i, weighting coefficient ω_i and the number of finite terms n. The parameters of FMN distributions are the mean and variance of the random wind speed μ_j, σ_j, weighting parameter α_j and the number of finite terms m. For the TNW distribution, the parameters include the scale and shape parameters α, β, weighting parameter ω_0 and random variables ϕ_1, ϕ_2. Besides,

the Weibull and Rayleigh distributions have been widely used for fitting the mainstream wind speed data. Such two distributions are also utilized for comparisons with non-parametric models. For the Weibull distribution, there are usually two parameters: scale parameter η and shape parameter β. For the Rayleigh distribution, the shape parameter σ should be determined.

The EM algorithm is utilized for the distribution parameter estimates of parametric models (AG, JW-TNW and JW-FMN). After numerical simulations, one can find that the high order terms of the FMvM and FMN distributions have little contributions to the fitting accuracy. Thus, the numbers of finite terms in the two distributions are all set to be $n = m = 3$ in this study. The maximum likelihood estimates for parametric models at various wind sites are given in Tabs. 2-4. It should be noted that the FMvM distributions used in the JW-TNW and JW-FMN models for the same wind direction data remain unchanged. Thus, parameter values of the FMvM for wind direction data are omitted in Tab. 4. In addition, the parameters values for both Weibull and Rayleigh distributions are also listed in Tab. 5.

Table 2

Parameter estimation results for the AG model at various wind sites (Units: m/s).

	AH site	GD site	GS site	HLJ site
$\mu_{y'}$	1.73149	3.72496	0.47598	5.25752
$\sigma_{x'}$	3.47676	4.07760	6.59563	2.23973
$\sigma_{y'}$	3.27303	4.29564	2.88817	5.74009

Table 3

Parameter estimation results for the JW-TNW model at various wind sites (Units: μ_i, μ_i^* (rad); $\phi_1, \phi_2, \alpha, \beta$ (m/s)).

		AH site	GD site	GS site	HLJ site
FMvM (direction)	$\omega_1, \mu_1, \kappa_1$	0.29290, 4.29805, 0.51945	0.64982, 0.11954, 64.40694	0.36226, 4.74585, 7.40989	0.75543, 4.41194, 14.85419
	$\omega_2, \mu_2, \kappa_2$	0.45144, 0.93909, 1.70044	0.03364, 0.59240, 261.37665	0.30449, 1.20769, 0.45863	0.18224, 0.96374, 39.05120
	$\omega_3, \mu_3, \kappa_3$	0.25566, 1.93091, 2.71713	0.31654, 2.22884, 2.78227	0.33325, 1.44542, 22.79816	0.06233, 0.68441, 0.57504
FMvM (circular variable)	$\omega_1^*, \mu_1^*, \kappa_1^*$	0.33463, 5.57145, 0.70241	0.36985, 4.05187, 0.90857	0.35466, 4.34628, 1.32540	0.34050, 4.9147, 0.52891
	$\omega_2^*, \mu_2^*, \kappa_2^*$	0.39724, 1.47754, 0.33603	0.38907, 6.13888, 0.73594	0.43896, 0.83888, 1.80479	0.44433, 0.28209, 1.39478
	$\omega_3^*, \mu_3^*, \kappa_3^*$	0.26813, 2.12253, 0.96998	0.24107, 2.47725, 0.93990	0.20637, 2.90370, 1.36813	0.21516, 3.23675, 1.56882
TNW (wind speed)	ω_0	0.46635	0.11459	0.30522	0.99402
	ϕ_1, ϕ_2	4.95522, 2.36729	4.93560, 5.26753	8.11738, 5.29833	7.16004, 3.63003
	α, β	3.81495, 4.92681	2.98356, 7.24868	2.11900, 5.64529	0.10701, 0.00006

Table 4

Parameter estimation results for the JW-FMN model at various wind sites (Units: μ_i^* (rad); μ_i, σ_i (m/s)).

		AH site	GD site	GS site	HLJ site
FMvM (circular variable)	$\omega_1^*, \mu_1^*, \kappa_1^*$	0.33599, 5.52568, 0.71352	0.35572, 4.46802, 0.81217	0.34971, 4.32000, 1.33454	0.35572, 4.46802, 0.81217
	$\omega_2^*, \mu_2^*, \kappa_2^*$	0.39895, 1.41515, 0.39336	0.43118, 0.30052, 1.75250	0.44212, 0.80302, 1.74510	0.43118, 0.30052, 1.75250
	$\omega_3^*, \mu_3^*, \kappa_3^*$	0.26507, 2.16453, 0.94977	0.21310, 3.00967, 1.31362	0.20817, 2.85487, 1.35154	0.21310, 3.00967, 1.31362
FMN (wind speed)	$\alpha_1, \mu_1, \sigma_1$	0.00562, 0.23834, 0.19524	0.01833, 0.24561, 0.21974	0.28157, 2.86599, 1.20855	0.01833, 0.24561, 0.21974
	$\alpha_2, \mu_2, \sigma_2$	0.84490, 4.47251, 1.53245	0.13275, 2.63963, 1.10383	0.52193, 6.07800, 2.18040	0.13275, 2.63963, 1.10383
	$\alpha_3, \mu_3, \sigma_3$	0.14948, 6.40896, 2.26980	0.84892, 8.21647, 2.91083	0.19650, 11.11342, 4.09700	0.84892, 8.21647, 2.91083

Table 5

Parameter estimation results for the Weibull and Rayleigh distributions at various wind sites (Units: η, β (m/s) and σ (m/s)).

		AH site	GD site	GS site	HLJ site
Weibull	η, β	2.598739, 5.268372	2.617606, 7.283343	1.723109, 6.928555	1.930503, 8.053095
Rayleigh	σ	3.591349	4.94729	5.101668	5.726812

4.2 Non-parametric models

Using two CV methods described in Eqs. (5-6), the optimal bandwidth values for the NP-KD and NP-JW models are determined accordingly. The results are listed in Tabs. 6-7.

Table 6

Bandwidth values for the NP-KD model at various wind sites.

	AH site	GD site	GS site	HLJ site
Gaussian bandwidth	0.42940	0.66170	0.65818	0.5997887
von Mises bandwidth	138.3239	708.9999	130.9623	204.5325

Table 7

Bandwidth values for the NP-JW model at various wind sites.

	AH site	GD site	GS site	HLJ site
Gaussian bandwidth	0.22354	0.19238	0.38974	0.28690
von Mises bandwidth (wind direction)	191.8563	709	266.1224	256.6935
von Mises bandwidth (circular variable)	14.7	11.6	17.4	23.001

5 Comparisons and discussions

Utilizing both parametric (AG,JW-TNW,JW-FMN,Weibull,Rayleigh) and non-parametric (NP-KD,NP-JW) models, the joint and marginal speed and direction distributions at AH station are shown in Figs. 3-4. The same plots are represented in Figs. 5-6, Figs. 7-8 and Figs. 9-10, but for the GD, GS and HLJ stations, respectively. From Figs. 3, 5, 7 and 9, one can see that the joint distribution curves fitted by parametric models seem to be more smooth, while the curves obtained by non-parametric models have some ups and downs besides the main peaks. This means that the non-parametric models could better capture the fluctuating components in the wind speed/direction change. Thus, the non-parametric might have superior fitting accuracy. For the marginal speed (or direction) distributions, as shown in Figs. 4, 6, 8 and 10, one can find that non-parametric models seem to be more suitable for fitting the actual wind speed (or direction) data, while the parametric models show less suit-

able, especially for the AG model. For the marginal direction data, it is shown that the result of AG model has much more distinct difference with that of JW-TNW and JW-FMN models. For the marginal speed data, among the five parametric models (AG,JW-TNW,JW-FMN,Weibull and Rayleigh), the accuracy of JW-TNW and JW-FMN models seems to be better, followed by the Weibull and Rayleigh models, and the AG model is the worst.

In order to quantitatively compare the fitting performance of various models, the RMSE,MAE,IA and χ^2 statistic for both joint and marginal PDFs at various wind stations are computed and listed in Tabs. 8-11. It is indicated that:

(1) The accuracy of JW-TNW is slightly better than that of the JW-FMN at the AH and GD sites (see Tabs. 8 and 9), while the opposite is true at the GS and HLJ sites (see Tabs. 10 and 11). Except for the HLJ site, in other three sites, the Weibull model has better performance in fitting the marginal speed distribution than the Rayleigh model. The performance of the AG model seems to be the worst among the parametric models.

(2) The non-parametric models (NP-JW,NP-KD) generally outperform the parametric models (AG,JW-TNW,JW-FMN,Weibull,Rayleigh) and have more robust fitting performance. Compared with the RMSE of the parametric and non-parametric models, the maximum accuracy increase appears at the GD site (see Tab. 9), which is increased from 8.82E-05 of the JW-TNW model to 7.66E-05 of the NP-KD model. The accuracy is increased by 13.1%. For the MAE metric, the maximum increase in accuracy also occurs at GD site (see Tab. 9), up from 1.87E-05 of the JW-TNW model to 1.66E-05 of the NP-KD model, with a relative decline of 11.2%. For the IA metric, the maximum in-

crease in accuracy appears at GD site (see Tab. 9), up from 6.43E-01 of the JW-TNW model to 7.63E-01 of the NP-KD model, with a relative increase of 18.7%. For the χ^2 statistic, the maximum increase in accuracy occurs at HLJ site (see Tab. 11), up from 2.56E+06 of the JW-FMN model to 5.56E+05 of the NP-KD model, with a relative increase of 78.3%. Similar phenomena could also be observed in the marginal speed or direction distributions.

(3) The NP-KD model has better performance in fitting joint distribution, while the NP-JW model has higher accuracy in fitting the marginal speed (or direction) distributions. This is because the bandwidth of NP-KD model is optimized globally, and it can more accurately describe the correlation between the wind speed and direction. In the NP-JW model, the bandwidths for the Gaussian and von Mises kernels are selected separately, and thus it might be more precious in fitting the marginal distributions. Thus, the NP-KD model would be a better choice for fitting the joint wind speed/direction distributions.

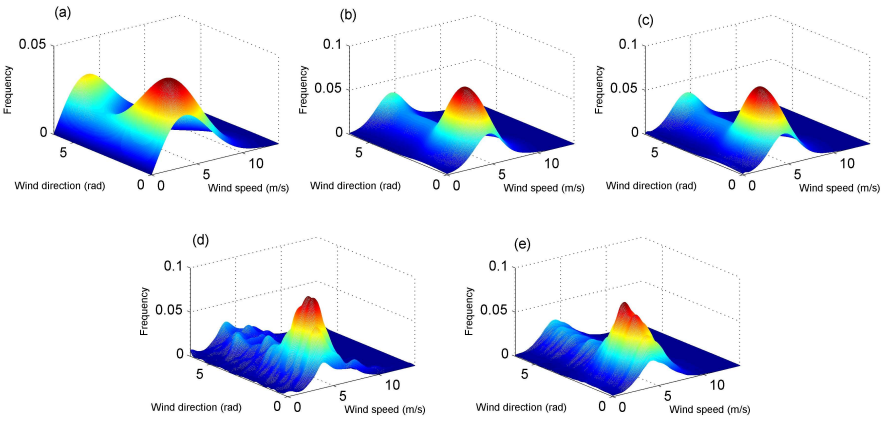

Fig. 3. Joint PDF plots at AH site: (a) AG model; (b) JW-TNW model; (c) JW-FMN model; (d) NP-KD model; and (e) NP-JW model.

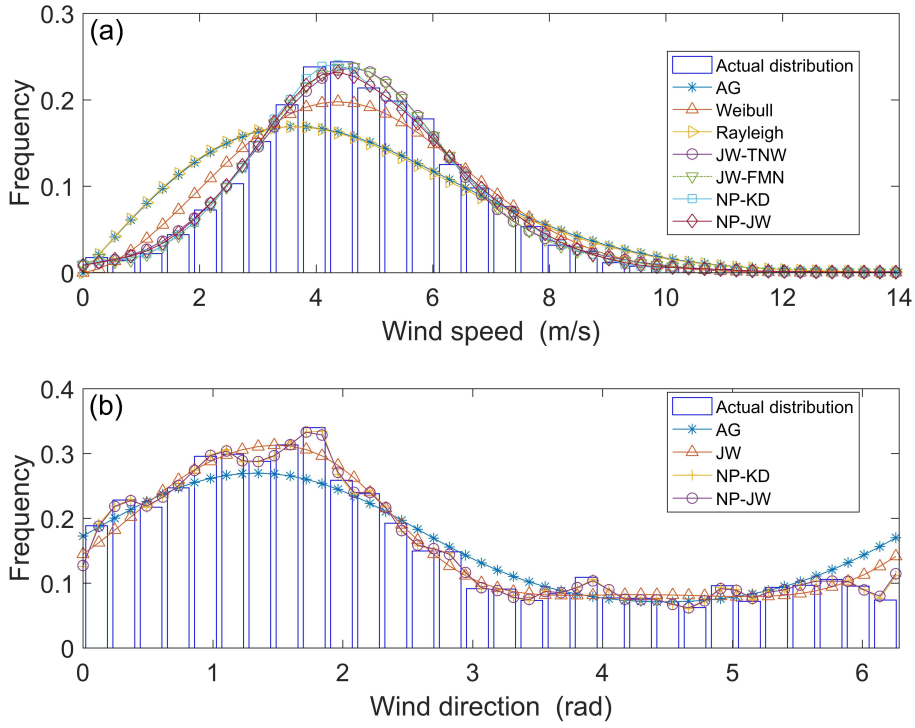

Fig. 4. Marginal PDF plots of wind speed (a) and direction (b) at AH site.

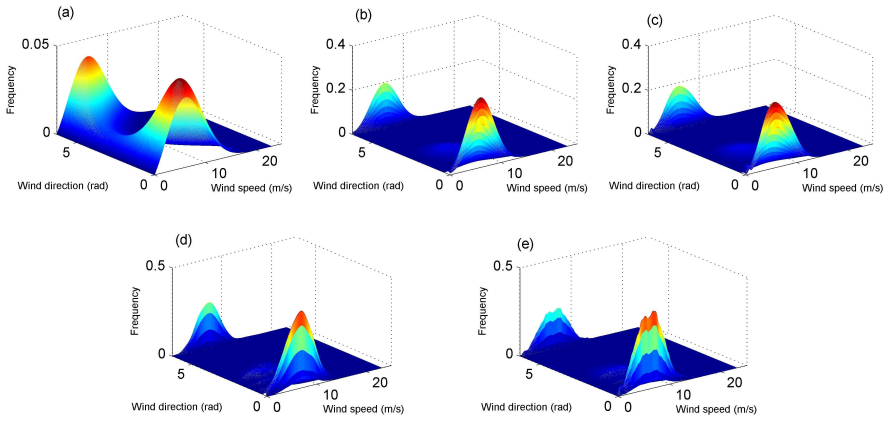

Fig. 5. Joint PDF plots at GD site: (a) AG model; (b) JW-TNW model; (c) JW-FM-N model; (d) NP-KD model; and (e) NP-JW model.

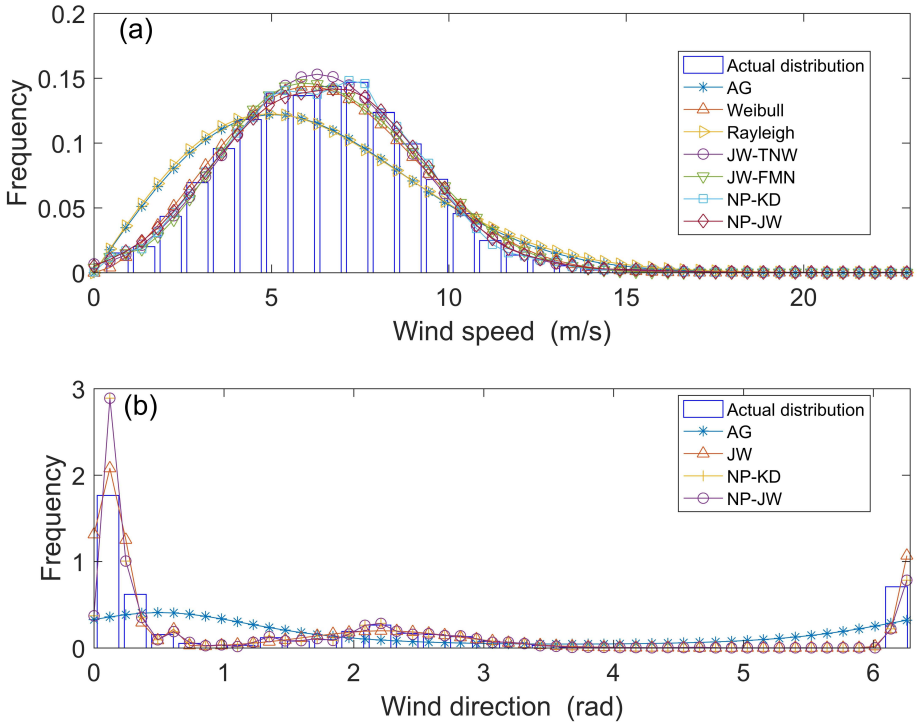

Fig. 6. Marginal PDF plots of wind speed (a) and direction (b) at GD site.

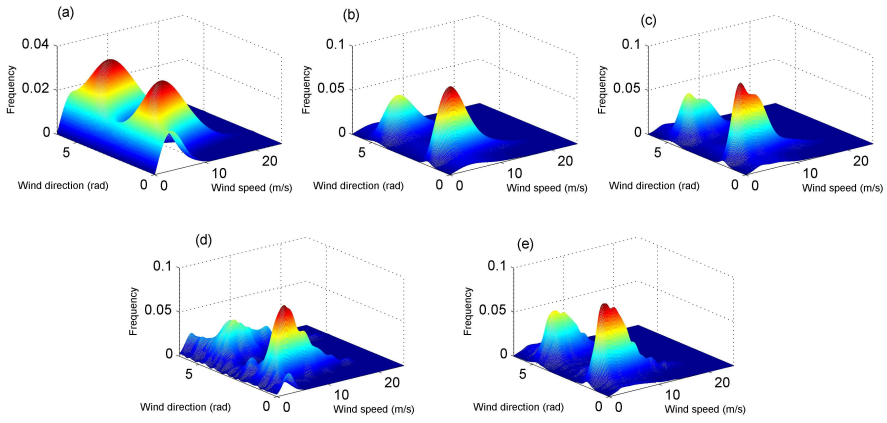

Fig. 7. Joint PDF plots at GS site: (a) AG model; (b) JW-TNW model; (c) JW-FMN model; (d) NP-KD model; and (e) NP-JW model.

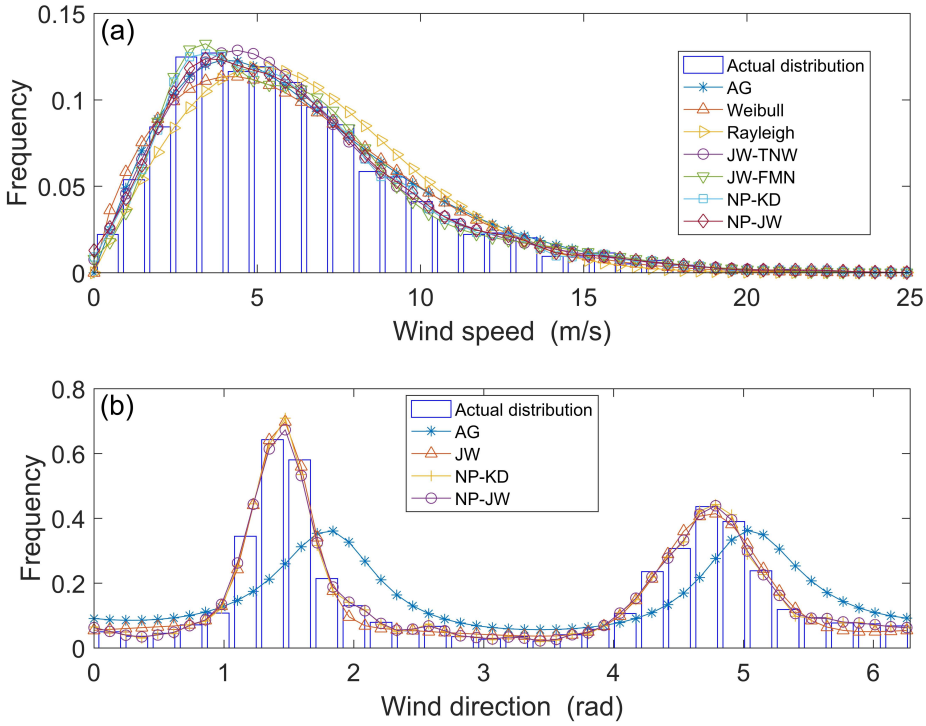

Fig. 8. Marginal PDF plots of wind speed (a) and direction (b) at GS site.

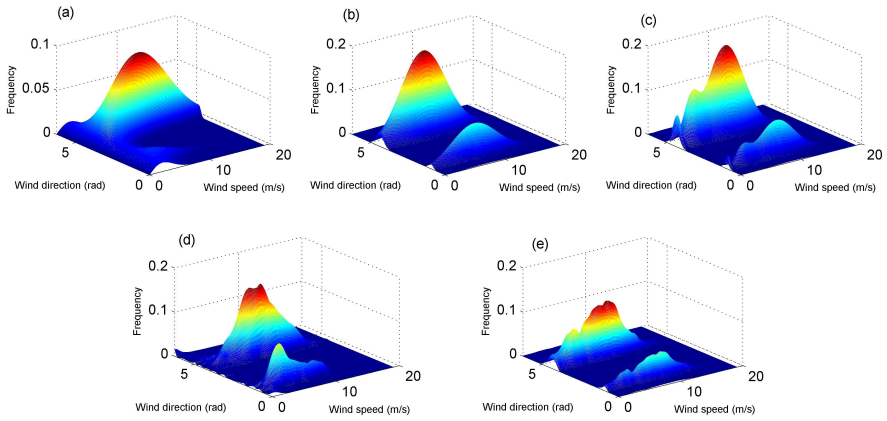

Fig. 9. Joint PDF plots at HLJ site: (a) AG model; (b) JW-TNW model; (c) JW-FM-N model; (d) NP-KD model; and (e) NP-JW model.

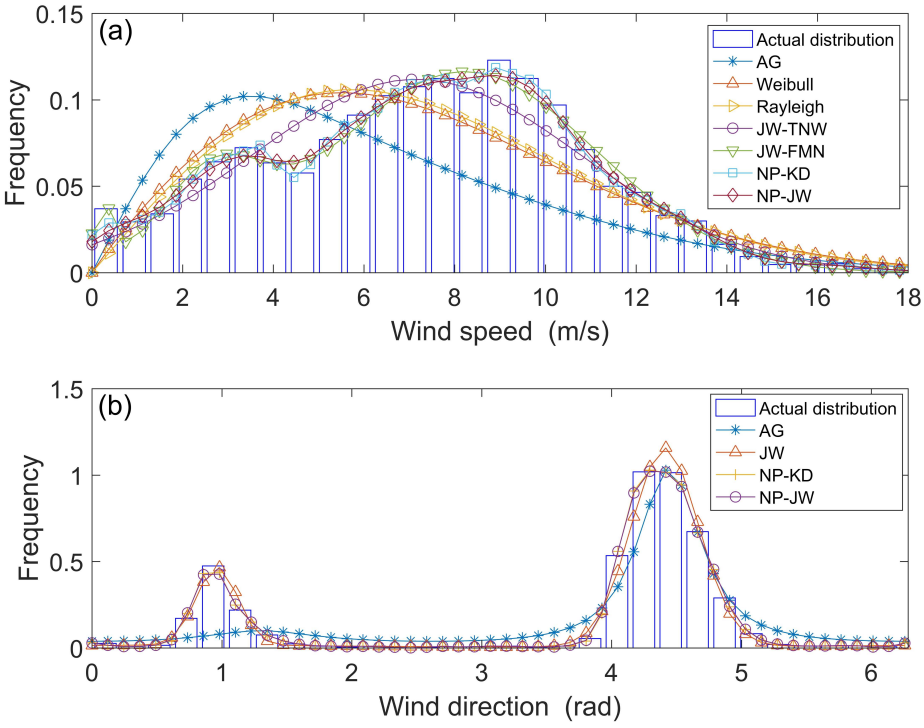

Fig. 10. Marginal PDF plots of wind speed (a) and direction (b) at HLJ site.

Table 8

RMSE,MAE,IA and χ^2 statistic for both joint and marginal PDFs at AH site.

		AG	Weibull	Rayleigh	JW-TNW	JW-FMN	NP-JW	NP-KD
Direction	RMSE	1.07E-03	-	-	9.03E-04	9.03E-04	7.34E-04	7.49E-04
	MAE	8.19E-04	-	-	6.95E-04	6.95E-04	5.65E-04	5.78E-04
	IA	9.27E-01	-	-	9.57E-01	9.57E-01	9.72E-01	9.71E-01
	χ^2	1.79E+01	-	-	1.37E+01	1.37E+01	8.56E+00	8.95E+00
Speed	RMSE	2.15E-03	1.20E-03	2.19E-03	7.92E-04	7.62E-04	7.02E-04	7.38E-04
	MAE	1.50E-03	7.72E-04	1.51E-03	5.22E-04	5.01E-04	4.45E-04	4.61E-04
	IA	9.21E-01	9.80E-01	9.18E-01	9.92E-01	9.93E-01	9.94E-01	9.93E-01
	χ^2	6.15E+01	2.68E+02	6.23E+01	1.77E+01	1.33E+01	8.66E+00	9.61E+00
Joint	RMSE	4.97E-05	-	-	4.64E-05	4.63E-05	4.64E-05	4.59E-05
	MAE	2.51E-05	-	-	2.23E-05	2.22E-05	2.24E-05	2.19E-05
	IA	3.37E-01	-	-	5.19E-01	5.23E-01	5.14E-01	5.36E-01
	χ^2	8.70E+05	-	-	1.30E+06	1.00E+06	7.09E+05	4.08E+05

Table 9

RMSE,MAE,IA and χ^2 statistic for both joint and marginal PDFs at GD site.

		AG	Weibull	Rayleigh	JW-TNW	JW-FMN	NP-JW	NP-KD
Direction	RMSE	1.47E-02	-	-	1.22E-02	1.22E-02	1.03E-02	1.03E-02
	MAE	4.93E-03	-	-	2.85E-03	2.85E-03	2.27E-03	2.27E-03
	IA	2.12E-01	-	-	6.92E-01	6.92E-01	8.06E-01	8.06E-01
	χ^2	1.75E+03	-	-	3.59E+02	3.59E+02	1.78E+02	1.78E+02
Speed	RMSE	1.81E-03	8.85E-04	1.87E-03	8.12E-04	8.41E-04	6.91E-04	7.59E-04
	MAE	1.16E-03	5.51E-04	1.23E-03	4.98E-04	5.18E-04	4.11E-04	4.66E-04
	IA	9.57E-01	9.91E-01	9.54E-01	9.93E-01	9.92E-01	9.95E-01	9.94E-01
	χ^2	4.99E+01	1.83E+04	4.17E+01	1.20E+01	1.63E+01	6.00E+00	8.58E+00
Joint	RMSE	1.02E-04	-	-	8.82E-05	8.83E-05	7.78E-05	7.66E-05
	MAE	2.55E-05	-	-	1.87E-05	1.88E-05	1.71E-05	1.66E-05
	IA	2.44E-01	-	-	6.43E-01	6.39E-01	7.53E-01	7.63E-01
	χ^2	1.45E+08	-	-	6.30E+05	5.63E+05	3.65E+05	1.81E+05

Table 10

RMSE,MAE,IA and χ^2 statistic for both joint and marginal PDFs at GS site.

		AG	Weibull	Rayleigh	JW-TNW	JW-FMN	NP-JW	NP-KD
Direction	RMSE	3.50E-03	-	-	1.13E-03	1.13E-03	9.73E-04	1.05E-03
	MAE	2.46E-03	-	-	8.28E-04	8.28E-04	6.66E-04	7.09E-04
	IA	6.72E-01	-	-	9.81E-01	9.81E-01	9.86E-01	9.84E-01
	χ^2	1.57E+02	-	-	2.48E+01	2.48E+01	1.53E+01	1.75E+01
Speed	RMSE	1.14E-03	1.25E-03	1.44E-03	1.10E-03	1.06E-03	9.89E-04	1.04E-03
	MAE	7.75E-04	8.46E-04	9.62E-04	7.34E-04	6.92E-04	6.50E-04	6.86E-04
	IA	9.82E-01	9.78E-01	9.72E-01	9.84E-01	9.85E-01	9.87E-01	9.85E-01
	χ^2	2.39E+01	3.38E+01	1.11E+02	2.22E+01	2.53E+01	1.78E+01	1.92E+01
Joint	RMSE	7.16E-05	-	-	7.12E-05	7.12E-05	7.11E-05	6.96E-05
	MAE	2.63E-05	-	-	2.51E-05	2.50E-05	2.51E-05	2.45E-05
	IA	3.39E-01	-	-	4.18E-01	4.16E-01	4.13E-01	4.51E-01
	χ^2	6.85E+05	-	-	9.26E+05	1.03E+06	9.01E+05	5.30E+05

Table 11

RMSE,MAE,IA and χ^2 statistic for both joint and marginal PDFs at HLJ site.

		AG	Weibull	Rayleigh	JW-TNW	JW-FMN	NP-JW	NP-KD
Direction	RMSE	3.06E-03	-	-	1.53E-03	1.53E-03	1.07E-03	1.11E-03
	MAE	2.05E-03	-	-	8.49E-04	8.49E-04	6.15E-04	6.39E-04
	IA	9.42E-01	-	-	9.88E-01	9.88E-01	9.94E-01	9.94E-01
	χ^2	2.26E+02	-	-	3.46E+01	3.46E+01	1.87E+01	1.98E+01
Speed	RMSE	2.72E-03	1.93E-03	1.87E-03	1.43E-03	1.27E-03	1.20E-03	1.25E-03
	MAE	1.97E-03	1.35E-03	1.30E-03	1.00E-03	8.80E-04	8.17E-04	8.54E-04
	IA	7.42E-01	8.80E-01	8.90E-01	9.41e-01	9.54E-01	9.60E-01	9.56E-01
	χ^2	2.26E+02	1.65E+02	2.10E+02	3.00E+01	3.40E+01	2.58E+01	2.96E+01
Joint	RMSE	9.36E-05	-	-	7.90E-05	7.88E-05	7.88E-05	7.64E-05
	MAE	2.99E-05	-	-	2.33E-05	2.32E-05	2.36E-05	2.20E-05
	IA	6.73E-02	-	-	5.04E-01	5.10E-01	4.94E-01	5.63E-01
	χ^2	7.39E+14	-	-	2.87E+06	2.56E+06	2.34E+06	5.56E+05

6 Conclusions

Two non-parametric models, namely the NP-KD and NP-JW models, are proposed to fit joint wind speed and direction distributions. The CV method is utilized for optimal bandwidth selections. Several classical parametric models, including the AG, Weibull, Rayleigh, JW-TNW and JW-FMN models, are also introduced in order for comparisons with the proposed non-parametric models. Through conducting various tests on the real hourly wind speed and direction data, the goodness of fit of both parametric and non-parametric models is compared and evaluated in detail. Some conclusions are summarized

as follows:

(1) It is shown that the proposed non-parametric models (NP-JW,NP-KD) generally outperform the parametric models (AG,Weibull,Rayleigh,JW-TNW,JW-FMN) and have more robust performance in fitting the joint speed and direction distributions.

(2) Among the two non-parametric models, the NP-KD model has better performance in fitting joint distribution, while the NP-JW model has higher accuracy in fitting the marginal speed (or direction) distributions.

(3) The NP-KD model would be a better choice for fitting the joint wind speed and direction distributions.

Acknowledgments

The research work described in the paper was supported by the National Science Foundation of China under Grant No. 51335006/11472147, and the State Key Laboratory of Tribology under Grant No. SKLT2015B12. Tao Hu's work was partly supported by the National Science Foundation of China under Grant No. 11671274/11471223 and Support Project of High-level Teachers in Beijing Municipal Universities in the Period of 13th Five-year Plan(No. CIT&TCD 201804078).

References

[1] Liu J, Ren G, Wan J, et al. Variogram time-series analysis of wind speed. Renewable Energy 2016;99:483-491.

[2] Sun C, Bie Z, Xie M, et al. Fuzzy copula model for wind speed correlation and its application in wind curtailment evaluation. Renewable Energy 2016;93:68-76.

[3] Petrovi V, Bottasso CL. Wind turbine envelope protection control over the full wind speed range. Renewable Energy 2017; 111: 836-848.

[4] Burton T, Sharpe D, Jenkins N, Bossanyi E. Wind Energy Handbook. John Wiley & Sons: Chichester, UK, 2001.

[5] Luna RE, Church HW. Estimation of long term concentrations using a universal wind speed distribution. Journal of Applied Meteorology 1974; 13: 910C916.

[6] Van der Auwera L, Meyer FD, Malet LM, The use of the Weibull three parameter model for estimating mean wind power densities. Journal of Applied Meteorology 1980;19:819C825.

[7] Bardsley WE. Note on the use of the inverse Gaussian distribution for wind energy applications. Journal of Applied Meteorology 1980; 19: 1126C1130.

[8] Li G, Shi J. Application of Bayesian model averaging in modeling long-term wind speed distributions. Renewable Energy 2010; 35: 1192-1202.

[9] Carta J A, Velazquez S. A new probabilistic method to estimate the long-term wind speed characteristics at a potential wind energy conversion site. Energy 2011; 36(5): 2671-2685.

[10] Soukissian T. Use of multi-parameter distributions for offshore wind speed modeling: the Johnson SB distribution. Applied energy 2013; 111: 982-1000.

[11] Shin J Y, Ouarda T B M J, Lee T. Heterogeneous mixture distributions for modeling wind speed, application to the UAE. Renewable Energy 2016; 91: 40-52.

[12] Hu Q, Wang Y, Xie Z, Zhu P, Yu D. On estimating uncertainty of wind energy with mixture of distributions. Energy 2016; 112: 935-962.

[13] Carta J A, Ramirez P, Velazquez S. A review of wind speed probability distributions used in wind energy analysis: Case studies in the Canary Islands. Renewable and Sustainable Energy Reviews 2009; 13(5): 933-955.

[14] Zhou J, Erdem E, Li G, Shi J. Comprehensive evaluation of wind speed distribution models: a case study for North Dakota sites. Energy Conversion and Management 2010; 51: 1449C1458.

[15] Ouarda T, Charron C, Chebana F. Review of criteria for the selection of probability distributions for wind speed data and introduction of the moment and L-moment ratio diagram methods, with a case study. Energy Conversion and Management 2016; 124: 247-265.

[16] Fisher NI. Statistical Analysis of Circular Data. Cambridge University Press: Cambridge, UK, 1993.

[17] Carta JA, Bueno C, Ramirez P. Statistical modelling of directional wind speeds using mixtures of von Mises distributions: case study. Energy Conversion and Management 2008; 49: 897C907.

[18] Masseran N, Razali A M, Ibrahim K, et al. Fitting a mixture of von Mises distributions in order to model data on wind direction in Peninsular Malaysia. Energy Conversion and Management 2013; 72: 94-102.

[19] Masseran N, Razali A M. Modeling the wind direction behaviors during the monsoon seasons in Peninsular Malaysia. Renewable and Sustainable Energy Reviews, 2016; 56: 1419-1430.

[20] Masseran N, Razali A M, Ibrahim K, et al. Fitting a circular distribution based on nonnegative trigonometric sums for wind direction in Malaysia. AIP Conference Proceedings 2015; 1643(1): 305-311.

[21] Marek J, Heckenbergerova J. Expectation-maximization algorithm for evaluation of wind direction characteristics. IEEE 15th International Conference

on Environment and Electrical Engineering (EEEIC), 2015: 1730-1735.

[22] Heckenbergerova J, Musilek P, Kr?mer P. Optimization of wind direction distribution parameters using particle swarm optimization. Afro-European Conference for Industrial Advancement. Springer International Publishing, 2015: 15-26.

[23] Bandte O, Mavris D N, DeLaurentis D A. Viable designs through a joint probabilistic estimation technique. World aviation congress and exposition, San Francisco. CA, October, 1999.

[24] Casella L. Improving long-term wind speed assessment using joint probability functions applied to three wind data sets. Wind Engineering 2012;36(4):473-483.

[25] Casella L. Performance analysis of the first method for long-term turbulence intensity estimation at potential wind energy sites. Renewable Energy 2015;74: 106-115.

[26] Smith OE. An application of distributions derived from the bivariate normal density function. Proceedings of International Symposium on Probability and Statistics in Atmospheric Sciences, Honolulu, 1971; 162C168.

[27] Weber R. Estimator for the standard deviation of wind direction based on moments of the Cartesian components. Journal of Applied Meteorology 1991;30:1341C53.

[28] Johnson RA, Wehrly TE. Some angularClinear distributions and related regression models. Journal of American Statistical Association 1978;73:602C6.

[29] Carta J A, Ramirez P, Bueno C. A joint probability density function of wind speed and direction for wind energy analysis. Energy Conversion and Management 2008;49(6):1309-1320.

[30] Erdem E, Shi J. Comparison of bivariate distribution construction approaches for analysing wind speed and direction data. Wind Energy 2011; 14(1): 27-41.

[31] Soukissian T H. Probabilistic modeling of directional and linear characteristics of wind and sea states. Ocean Engineering 2014; 91: 91-110.

[32] Soukissian T H, Karathanasi F E. On the selection of bivariate parametric models for wind data. Applied Energy 2017; 188: 280-304.

[33] Wang J, Hu J, Ma K. Wind speed probability distribution estimation and wind energy assessment. Renewable and Sustainable Energy Reviews 2016; 60: 881-899.

[34] Qin Z, Li W, Xiong X. Estimating wind speed probability distribution using kernel density method. Electric Power Systems Research 2011; 81(12): 2139-2146.

[35] Xu X, Yan Z, Xu S. Estimating wind speed probability distribution by diffusion-based kernel density method. Electric Power Systems Research 2015; 121: 28-37.

[36] Ouarda T, Charron C, Shin J Y, Marpu P Y, Al-Mandoos A H, Al-Tamimi M H, Ghedira H, Al Hosary A H. Probability distributions of wind speed in the UAE. Energy Conversion and Management 2015; 93: 414-434.

[37] Oliveira M, Crujeiras RM, Rodriguez-Casal A. NPCirc: An R package for nonparametric circular methods. Journal of Statistical Software 2014; 61(9): 1-26.

[38] Zhang J, Chowdhury S, Messac A, et al. A multivariate and multimodal wind distribution model. Renewable Energy 2013; 51: 436-447.

[39] Zambom A Z, Dias R. A review of kernel density estimation with applications to econometrics. arXiv preprint arXiv:1212.2812, 2012.

[40] Oliveira M, Crujeiras RM, Rodrspguez-Casal A. Plug-in Rule for Bandwidth Selection in Circular Density Estimation. Computational Statistics & Data Analysis 2012;56(12):3898-3908.

[41] Banerjee A, Dhillon I S, Ghosh J, et al. Clustering on the unit hypersphere using von Mises-Fisher distributions. Journal of Machine Learning Research 2005; 6(Sep): 1345-1382.

[42] Calderara S, Prati A, Cucchiara R. Mixtures of von mises distributions for people trajectory shape analysis. IEEE Transactions on Circuits and Systems for Video Technology 2011; 21(4): 457-471.

[43] Yates F. Contingency tables involving small numbers and the chi2 test. Supplement to the Journal of the Royal Statistical Society 1934; 1(2): 217-235.

[44] Zar J H. Biostatistical Analysis. Prentice-Hall: Old Tappan, NJ, 1999.